Hyaluronan-modified Magnetic Hydroxyapatite Nanocrystals for Hyperthermia

H.-C. Wu*, S.-Y. Hsieh*, T.-W. Wang**

*Department of Materials Engineering, Tatung University
40 Zhongshan North Road, 3rd Section, Taipei City 104, Taiwan, hsichin.wu@gmail.com
**Department of Materials Science and Engineering, National Tsing Hua University, Hsinchu, Taiwan, twwang@mx.nthu.edu.tw

ABSTRACT

The success of tumor therapy is determined by the efficiency with which the killing of tumor cells is achieved under conditions of no or only slight damage to the normal tissues. Because of its high tumor specificity and biocompatibility, hyaluronic acid (HA) could be potentially used for the design of tumor-targeting marker. HA, one of the major components of vertebrate tissue and body fluid, has been known to interact with the hyaluronan receptor, CD44. HA-CD44 binding triggers intracellular signals that influence cellular proliferation, differentiation, and migration. In this study, HA modified magnetic hydroxyapatite (HA-modified mHAP) nanocrystals were newly developed and synthesized by wet chemical precipitation process. The result demonstrated that poly (ethylene glycol) (PEG) spacer arm and HA targeting moiety were successfully immobilized on the surface of mHAP. Moreover, HA-modified mHAP possessed relatively good biocompatibility, adequate biodegradation rate and superparamagnetic property. In summary, HA-modified mHAP could not only be localized in site, but also be used for the heat generation agent within applied external magnetic field. The results from this study indicate that the biocompatible HA-modified mHAP shows promise for use as novel heat mediator in future hyperthermia cancer therapy.

Keywords: bioceramic, hyperthermia cancer therapy, magnetic nanocrystal

1 INTRODUCTION

Cancer is one of major cause of death in the worldwide. There is still no standard treatment method for patients with malignant diseases inspite of the progress in the development of anticancer strategy. Challenges of cancer therapy rely on effective drug delivery and targeting systems, which can play a vital role to increase the therapeutic outcome while minimizing side effects[1].

Various superparamagnetic nanoparticles (NPs) such as magnetite have been widely used in biomedical applications including specific delivery and release therapeutic vehicle, enhanced contrast agent for magnetic resonance imaging (MRI) , and hyperthermia, etc[2]. For these applications, the internalization of nanoparticles into specific cells is the curcial step and necessary required features including prolong blood half-life, specific targeting, and high efficiency of internalization of endocytosed ligands grafted on the nanoparticles[3].

Hydroxyapatite (HAP) is similar to the main mineral component in human body and a well known biocompatible biomaterial for extensive bioengineering applications. Pervious study showed the novel synthesis of non-toxic magnetic-hydroxyapatite (mHAP) nanocrystal that could be incorporated into HAP with superparamagnetic properties[4]. In addition, it may greatly enhance the specific delivery of drugs by magnetic field and act as an in vivo traceable agent. However, NPs have the phenomenon of aggreagation and adsorption of plasma proteins due to large surface area/ volume ratio. Therfore, NPs are quickly cleaned by macrophages before reaching targeted sites. PEG surface modification has been proved one possible approach to increase the circulation time of NPs and minimize clearance in the blood stream[5]. Also, facilitation of vaild and specific cellular uptake of NPs is depending on the surface modification with a ligand that is efficiently taken up by target cells via receptor mediated endocytosis process. A lot of HA-binding receptors such as cell surface glycoprotein CD44 and receptor for HA-mediated motility (RHAMM) are commonly known for overexpression in various cancer. Therefore, covalently immobilizing HA on the surfaces of mHAP is expected to effectively improve the biocompatibility, binding efficiency and internalization into tumor cells[6].

In this study, PEG and HA were immobilized on the surfaces of mHAP nanocrystal for particles dispersion, better cell internalization , and cancer cells targeting. The uptake of the modified nanocrystals by mouse embryonic fibroblast cell line (3T3) and metastatic human breast cancer cell line (MDA-MB-231) was studied using unmodified nanocrystals as a control. The characterization of mHAP modification was determined by transmission electron microscope (TEM), Fourier transform infrared spectra (FTIR), thermogravimetric thermal analyzer (TGA), inductively coupled plasma emission spectroscopy (ICP), vibrating sample magnetometer (VSM), and optical microscopy.

2 EXPERIMENT

2.1 Synthesis and Surface Modification of mHAP Nanocrystals

The mHAP nanocrystals were prepared using controlled coprecipitation as reported previously[7]. The crystalss were collected by sedimentation with the external magnetic field and washed with deionized water.

Surface modification of mHAP was carried out via grafting to introduce amine groups (Figure 1(a)). In this study, CDI was anchored to the surface of mHAP. For grafting, 100 mg of mHAP was washed with DMSO. Then, mHAP were then dispersed into DMSO with CDI (33.2 mg/ mL), and the solution was heated to 60 °C, and the reaction was carried out for 2 hours under vigorous stirring. Thereafter, the same volume of PEG (167 mg/ mL) solution was added to the mHAP suspension. The suspension was further reacted at R.T. for 24 hours and vigorous stirring. The modified crystals were magnetically collected, washed with deionized water three times, and dried in a vacuum. For preparation of HA-modified mHAP (Figure 1(b)), the 4:1 (w/w) of EDC and NHS were added into HA (2.5 mg/ mL) in 0.1M MES buffer, and then stirred for 10 min. PEG-mHAP (2.5 mg/ mL) were added into the mixture. The mixture was treated with ultrasonic for 10 min and stirred for following 24 hours. After the reaction, thecomposites were collected through magnetic separation and were washed by deionized water for several times. The products were dried at vacuum conditions.

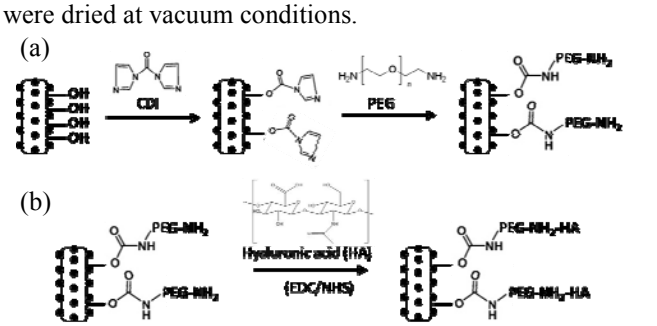

Figure 1: A schematic illustration for the formation of (a) PEG-mHAP and (b) HA-modified mHAP nanocrystal.

2.2 Characterization

The size, morphology of the synthesized HA-modified mHAP nanocrystals were analyzed using transmission electron microscope (TEM). Fourier Transform Infrared Spectroscopy (FTIR) was used to confirm the functional groups of the PEG and HA grafting. Scans between the wavelengths 4000 and 400 cm^{-1} were recorded using potassium bromide pellet method. The samples (~10 mg) were heated from room temperature to 1300 °C at a heating rate of 10 °C/ min in air by thermogravimetric thermal analyzer (TGA). Magnetic properties of magnetic nanocrystals were characterized by vibrating sample magnetometer (VSM). The heating experiments in AC magnetic field were performed in a medium frequency induction heating apparatus at room temperature. A optic fiber thermometer was used to record the temperature to avoid any electrical or magnetic heating of the temperature probe. Finally, the chemical composition of nanocrystals was analyzed by inductively coupled plasma mass spectrometry (ICP-MS)

2.3 Cell Culture, Labeling and Celluar Uptake

3T3 and MDA-MB-231 were purchased from the Bioresource Collection and Research Center. Cells were used in these experiments. Cells were routinely cultured at 37°C in a humidified atmosphere with 5% CO2 for 3T3 or in air for MDA-MB-231 with the growth medium changed twice every week, respectively. The cells were then allowed to grow to about 75% confluence before use. The cultured cells were dettached by trypsinization (0.25% trypsin-EDTA), suspended in a fresh culture medium and used for the further experiments described below.

Cell viability was determined through LDH assay. Each well of the 96-well culture plate was seeded with 5×10^3 3T3 cells. The cells were cultivated in 200 µl cultured medium. After 24 h of culture, the medium in the wells was refreshed with the medium containing HA-modified mHAP nanocrystals at a concentration ranging from 0 to 0.5 mg/ ml. The nanocrystals were cocultured with 3T3 cells for 1 and 3 days followed by further analysis.

For cell labeling, cell suspensions were seeded in a 12-well plate at a density of 5×10^4 cells/ well. After 24 h, the medium was aspirated and replaced with either a fresh medium or a medium with the nanocrystal at a concentration of 0.01 mg/ mL. The cells were cultured for another 1.5 h. The cells were then washed with phosphate buffered silane (PBS; pH 7.4) extensively to completely remove unattached and free particles in the medium before further experiments. Prussian Blue staining assay was used to study the cellular uptake of nanocrystals via optical microscopy. The cells after labeling were washed three times with PBS and subsequently fixed in 4% formaldehyde in PBS for 20 min. For Prussian Blue staining, cells were washed with PBS, incubated for 30 min with 5% potassium hexacyanoferrate (II) trihydrate in 5% HCl, washed with deionized water, and counter-stained with Nuclear Fast Red. The quantification of nanocrystals uptake into the cells was analysed by ICP-MS.

2.4 Statistical Analysis

All data were expressed as mean ± standard deviation, and were analysed by analysis of variance (one-way ANOVA). Statistical significance was accepted at a level of $p < 0.05$.

3 RESULTS

The XRD of mHAP, PEG-mHAP and HA-modified mHAP showed specific peaks corresponding to those of reference HAP and magnetite (JCPDS cards 9-432 and 19-

629) (data not shown). The HAP lattice was suggested to be intact and iron oxide was getting heterogeneous nucleation growth and accommodated in the interstitial spaces.

From the FTIR spectrum, there was a remarkable change in the peak of the C–O stretching band at 970 to 1250 cm^{-1} of PEG-mHAP. The presence of the amide band at 1630 to 1650 cm^{-1} was observed in HA-modified mHAP nanocrystals (Figure 2A). Moreover, the increasing of weight loss rate was increased with the amount of PEG and HA modified on the surface of mHAP nanocrystals according to the TGA results (Figure 2B). As a result, it was obvious that there were strong chemical interactions between PEG, HA and the nucleating mHAP nanocrystals.

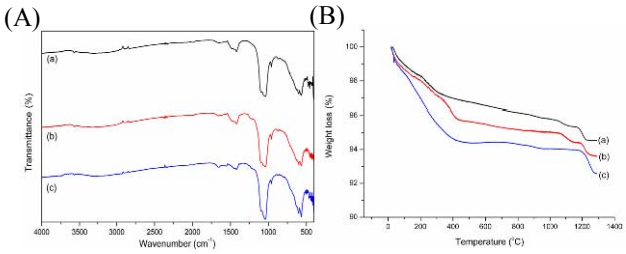

Figure 2: (A) FTIR spectra and (B) TGA analysis of (a) mHAP, (b) PEG-mHAP, (c) HA-modified mHAP.

The size of the individual HA-modified mHAP was rod-like shape around 100×40 nm from the TEM images (Figure 3), while the small particles (about 10 nm) were adhered surrounding the surface of spindle nanocrystal. The hydrodynamic size of the HA-modified mHAP was 428 nm. The larger hydrodynamic size may be due to some degree of aggregation of the nanocrystals as well as the contribution from the polymeric shell,which was hardly seen on the TEM images.

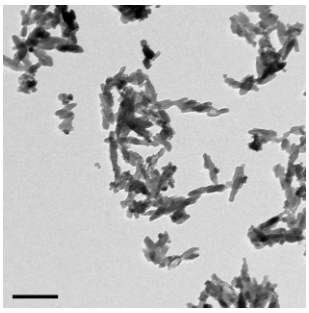

Figure 3: TEM image of HA-modified mHAP. Scale bar: 200 nm.

The magnetic hysteresis curves can be noticed that no coercivity or remanence was observed for all of the three samples. The mHAP nanocrystals were possessed with the superparamagnetic property (Figure 4A). This can be considered to have small size NPs which were smaller than the superparamagnetic critical size (25 nm)[8]. The saturation magnetization (Ms) of the mHAP, PEG-mHAP and HA-modifed mHAP was 33.4, 32.3 and 28.3 emu/g, respectively. The decrease in the Ms value could be explained by the presence of the nonmagnetic PEG and HA coating. However, the values of the Ms were sufficient for the application of hyperthermia.

The heating curves were shown in Figure 4B for different samples at fixed concentration (0.5 mg/mL) of mHAP, PEG-mHAP and HA-modifed mHAP. From the results, it can be seen that the bear mHAP nanocrystals have better heating efficiency than that of PEGF-mHAP and HA-modifed mHAP. The divergence temperature of mHAP could rise 7.7, 6.9 and 5.4 °C in 5 mins, respectively. The decrease of the heating effect could be attributed to the magnetization resuction due to the coating with PEG and HA.

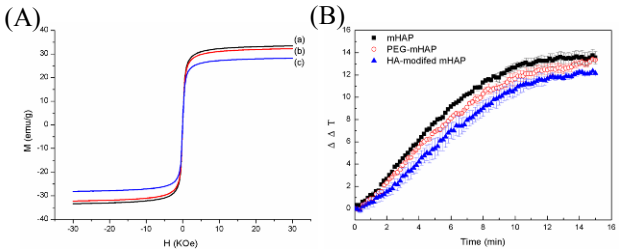

Figure 4: (A) Magnetic hysteresis curves at room temperature. (B) Heating generation ability in alternative magnetic filed for (a) mHAP (square), (b) PEG-mHAP (circular), and (c) HA-modified mHAP (triangle).

The viability of 3T3 after cocluture with nanocrystals was evaluated and compared to cells in the control experiment (no nanocrystal exist) using the LDH assay, which has been described as a method for the detection of cytotoxicity. For HA-modified mHAP, no significant cytotoxicity effect was observed within tested concentrations when compared to nontoxic control (Figure 5).

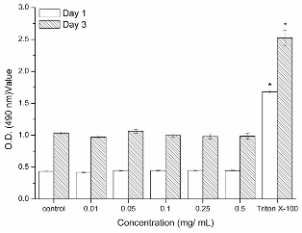

Figure 5: Viability of 3T3 grown in media containing 0 ot 0.5 mg/ mL of HA-modifed mHAP. Media without nanoparticles and with 1% Triton X-100 served as the nontoxic and toxic controls, respectively. Asterisks denote significant differences from the control ($P < 0.05$).

In general, surface modification is the common strategy to enhance the cellular uptake of nanoparticles. In this study, the surface of mHAP was modified with PEG and HA in order to promote the specific cellular uptake. Nanocrystal uptake by 3T3 and MDA-MB-231 was visualized using optical microscopy after the cells were grown in a medium with or without nanocrystals for 1.5 h. The cells were

stained with Prussian Blue for the specific detection of intra-cellularization. From Figure 6, the presence of blue particles in MDA-MB-231 cells can be observed when labeling was carried out with HA-modified mHAP, while it was much less with mHAP and PEG-mHAP and no blue particle was seen in the unlabeled cells. This intracellular uptake is desirable because nanocrystals on the cell membrane may be targeted or delivered to other cells in vivo. Furthermore, there was a possibility that membrane-bound crystals may interfere with receptor mediated endocytosis (membrane recognition processes). The amount of HA-modified mHAP uptake by MDA-MB-231 was much more than that of other groups. The quantification of iron uptake by ICP-MS as shown in Figure 7. HA-modified mHAP were rapidly internalized into the cells within the first hour. Due to PEG possessing with prolonged circulation time in plasma, the iron accumulation of PEG-mHAP was lower than that in HA-modified mHAP nanocrystal. In contrast, unlabeled cells exhibited an iron content of less than 1 pg/cell from the natural intracellular iron source.

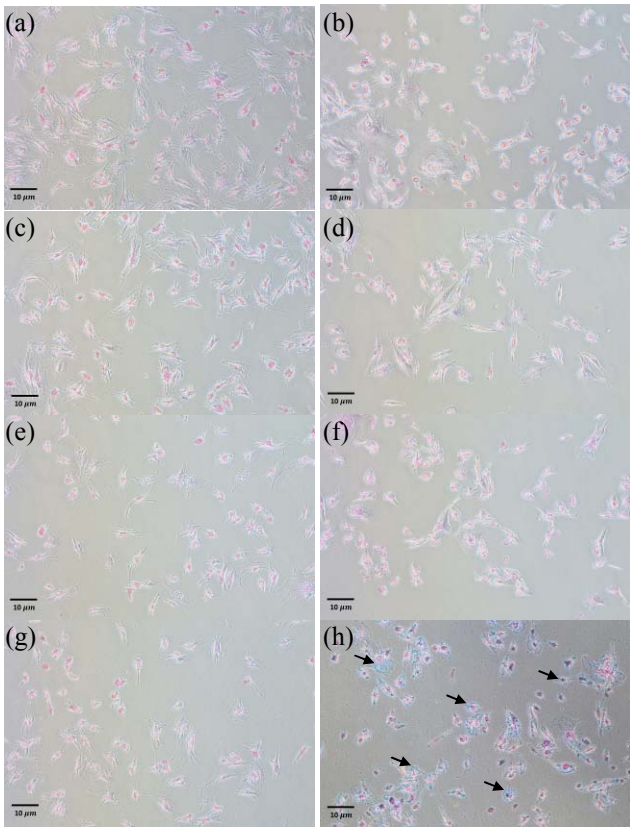

Figure 6: Representative Prussian Blue and Nuclear Fast Red counter staining of (a, c, e, g) 3T3 and (b, d, f, h) MDA-MB-231 cells that were incubated (a, b) without NPs, (c, d) with mHAP,with (e, f) PEG-mHAP and (g, h) with HA-modifed mHAP for 1.5 hours. 0.01 mg/mL mHAP, PEG-mHAP, HA-modified mHAP were used.

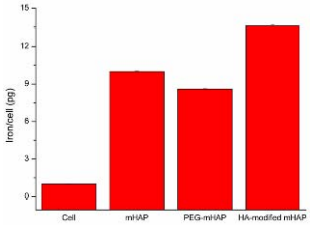

Figure 7: Cellular uptake of the HA-modified mHAP (0.01 mg/mL in medium) after incubation for 1 h.

4 CONCLUSION

The surface of mHAP was successfully conjugated to HA biopolymer through a PEG space arm linker. The enhanced intracellular uptake of HA-modified mHAP by 3T3 and MDA-MB-231 cell lines was confirmed by optical microscopy examination. It was also certained that there was no adverse effect on the cell viability after labeling with HA-modified mHAP. The preferential uptake of such nanocrystals by MDA-MB-231 was likely as a result of the high labeling efficiency of HA-modified mHAP. Besdies, the reactive group (-COOH) present on the HA-modified mHAP provides the opportunity for further functionalization of the surface. It is expected that a variety of other biomolecules may be immobilized onto the HA-modified mHAP to enhance specific cell recognition for targeting purposes. Thus, HA-modified mHAP is considered as a promising tool for the labeling of cancer cells for hyeprthermia therapeutic applications in medical cancer therapy.

REFERENCES

[1] L. Brannon-Peppas and J. O. Blanchette, Adv Drug Deliv Rev, vol. 56, pp. 1649-59, Sep 22 2004.
[2] J. Gao, et al., Acc Chem Res, vol. 42, pp. 1097-107, Aug 18 2009.
[3] S. Jaracz, et al., Bioorg Med Chem, vol. 13, pp. 5043-54, Sep 1 2005.
[4] H. C. Wu, et al., Nanotechnology, vol. 18, Apr 2007.
[5] Y. Zhang, et al., Biomaterials, vol. 23, pp. 1553-1561, Apr 2002.
[6] X. H. Peng, et al., Int J Nanomedicine, vol. 3, pp. 311-21, 2008.
[7] H. C. Wu, et al., Advanced Functional Materials, vol. 20, pp. 67-77, Jan 2010.
[8] P. Pradhan, et al., Journal of Biomedical Materials Research Part B-Applied Biomaterials, vol. 81B, pp. 12-22, Apr 2007.